Journal of Sound and Vibration (2001) **245**(1), 63–78
doi:10.1006/jsvi.2000.3543, available online at http://www.idealibrary.com on IDEAL®

BENDING AND FORCED VIBRATION RESPONSE OF A CLAMPED ORTHOTROPIC THICK PLATE AND SANDWICH PANEL

T. S. Lok

Nanyang Technological University, School of Civil and Structural Engineering, Nanyang Avenue, 639798 Singapore. E-mail: ctslok@ntu.edu.sg

AND

Q. H. Cheng

Institute of High Performance Computing, 89C Science Park Drive, 118261 Singapore

(*Received* 31 *May* 2000, *and in final form* 24 *November* 2000)

A closed-form solution for the forced response of an orthotropic thick plate and sandwich panel has been developed and is presented in this paper. The paper outlines the methodology and develops the formulation to enable the solution to be derived. A novel truss-core sandwich panel is introduced and a method is outlined in which the panel is represented as an equivalent homogeneous orthotropic thick plate continuum. The 3-D dynamic finite element method is one of the most versatile developments of the 20th century. However, the software is not as accessible or as user-friendly for engineers who are not trained in such analytical tools. Therefore, alternative methods of analysis must be found, especially in the dynamic assessment of thin-walled truss-core sandwich panels. One way is to transform the sandwich structure into an equivalent homogeneous orthotropic thick plate continuum and to conduct the analysis on the equivalent model. The authors have derived the necessary elastic constants to hasten this transformation. In this paper, the derived elastic constants are used with closed-form solution to determine the bending and forced vibration response of a clamped truss-core sandwich panel, represented as a homogeneous orthotropic thick plate continuum. The Rayleigh–Ritz method is employed for the closed-form solution and the forced response is determined using Duhamel's integral. Admissible functions are taken as a series of products of beam mode-shape functions in the two orthogonal directions. The beam function in either direction is derived from the corresponding beam eigenvalue problem. Numerical examples, which include the influence of transverse shear on the response, show that the closed-form solution agrees with analytical and numerical data available in the literature and also with 3-D finite element results.

1. INTRODUCTION

Structural sandwich panels are favored over other structural forms because they provide better stiffness and strength per unit weight. Plantema [1] has written about the topic and Libove and Hubka [2] and Fung *et al.* [3, 4] have thoroughly researched the various core configurations to highlight the benefits of such structural forms. A number of these thin-walled sandwich panels may be seen in Figure 1. Such sandwich panels have relatively high transverse shear deformation in one or both planes of bending, a result due almost

0022-460X/01/310063 + 16 $35.00/0

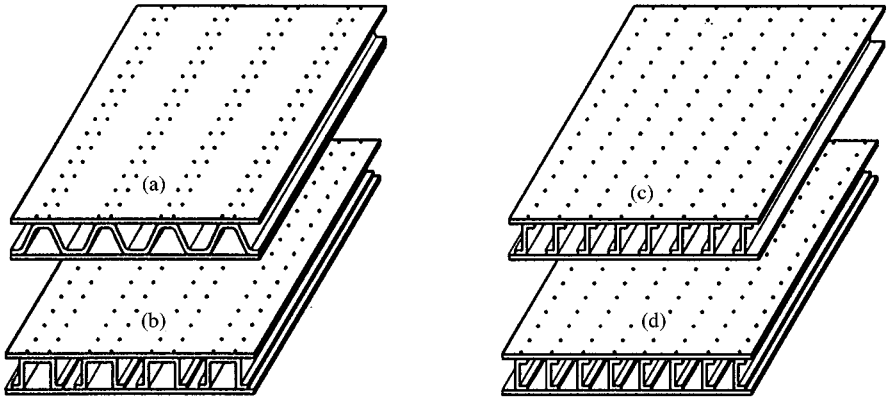

Figure 1. Thin-walled sandwich panels.

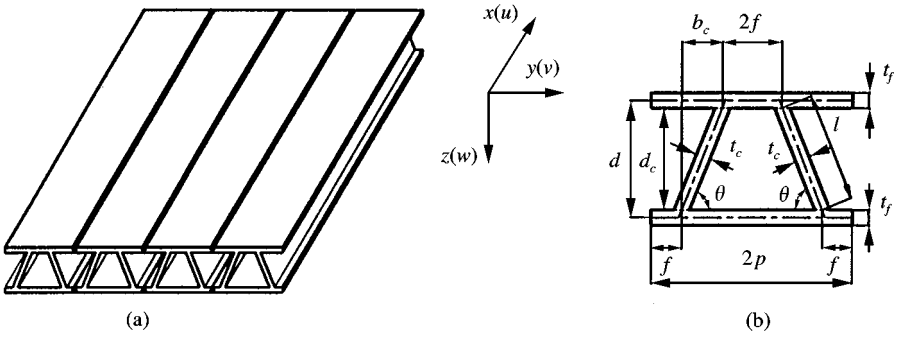

Figure 2. (a) Truss-core sandwich panel and (b) dimensions of a panel unit.

entirely to the characteristics of the core. This is not surprising because different core shapes and arrangements provide responses that vary significantly from one another.

Recent experience indicates that there is considerable difficulty in producing the panels shown in Figure 1 with an acceptable surface finish. The reliability of the connection is also questionable because proper attachment between the thin materials, either by fusion of the materials or by screws/rivets, cannot be guaranteed. The truss-core sandwich panel proposed by Lok and Cheng [5] and shown in Figure 2(a) has merit because each unit is a structural element. A number of these units may be positioned side-by-side and welded at the flanges to form a large sandwich panel. To reduce the number of joints, a wide section comprising a number of units could be extruded in one operation. Instead of welding, an additional thin sheet could be glued to the top and bottom faces of these units to form a rigid panel. Figure 2(b) shows the cross-section dimensions of a truss-core unit; the geometry of the section is completely described by these dimensions.

A 3-D thin-walled sandwich panel may be represented as an equivalent 2-D thick plate, which is continuous and homogeneous, and orthotropic with respect to the mutually perpendicular x and y directions. The authors have derived the necessary elastic constants for the truss-core sandwich panel, which is represented by bending, twisting and transverse stiffnesses and the Poisson ratio of a continuum. These constants are obtained by

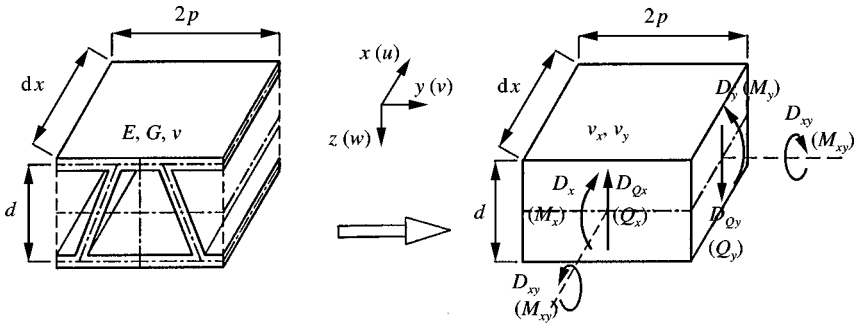

Figure 3. Transformation of a truss-core unit to a homogeneous, orthotropic thick plate continuum.

comparing the behavior of a unit thin-walled sandwich panel with that of an element of the thick plate, with all its attendant material properties, as shown in Figure 3. By incorporating the derived elastic constants and employing the Rayleigh–Ritz method, closed-form solutions were developed for bending [6] and free vibration analysis [7] of the truss-core sandwich panel.

In a previous article [7], several techniques and their corresponding merit in estimating the free response of thin and thick orthotropic plates and sandwich panels were highlighted. Laura and Duran [8] used simple polynomial approximations and Galerkin's method to determine the response of thin, rectangular clamped plates subjected to sinusoidal excitation. Difficulties encountered by a number of investigators prompted Ramkumar *et al.* [9] and Chen and Ramkumar [10] to develop the Lagrangian multiplier technique for the dynamic analysis of thick plates including the effects of transverse shear. However, one of the disadvantages of their solution is that when the number of the Lagrangian multiplier is smaller than the number of vibration modes to be computed, the mode shape functions may not completely satisfy the boundary conditions. Further, the solution gives zero bending moment on the edges of the clamped plate.

In this paper, a bending and forced vibration analysis is developed to assess the response of fully clamped orthotropic plates. The technique is presented in detail, together with a brief description of free vibration analysis by the mode superposition method. Several numerical examples are provided to verify the proposed method.

2. THEORETICAL DEVELOPMENT

2.1. GOVERNING DIFFERENTIAL EQUATIONS

A general, small-deflection theory developed by Libove and Batdorf [11] to describe the flexural behavior of orthotropic plates and sandwich panels is extended for dynamic analysis by including the mass and moment of inertia of the plate. The governing differential equations of the problem are

$$D_{Qx}\left(\frac{\partial^2 w}{\partial x^2} - \frac{\partial \theta_x}{\partial x}\right) + D_{Qy}\left(\frac{\partial^2 w}{\partial y^2} - \frac{\partial \theta_y}{\partial y}\right) + p = \rho h \frac{\partial^2 w}{\partial t^2}, \tag{1a}$$

$$D_{Qx}\left(\frac{\partial w}{\partial x} - \theta_x\right) + \frac{D_{xy}}{2}\left(\frac{\partial^2 \theta_x}{\partial y^2} + \frac{\partial^2 \theta_y}{\partial x \partial y}\right) + \frac{D_x}{g}\left(\frac{\partial^2 \theta_x}{\partial x^2} + \nu_y \frac{\partial^2 \theta_y}{\partial x \partial y}\right) = J_x \frac{\partial^2 \theta_x}{\partial t^2}, \tag{1b}$$

$$D_{Qy}\left(\frac{\partial w}{\partial y}-\theta_y\right)+\frac{D_{xy}}{2}\left(\frac{\partial^2\theta_y}{\partial x^2}+\frac{\partial^2\theta_x}{\partial x\partial y}\right)+\frac{D_y}{g}\left(\frac{\partial^2\theta_y}{\partial y^2}+v_x\frac{\partial^2\theta_x}{\partial x\partial y}\right)=J_y\frac{\partial^2\theta_y}{\partial t^2}, \tag{1c}$$

where $g = 1 - v_x v_y$; $p = p(x, y, t)$ is the lateral dynamic load acting on the surface of the plate; w is the displacement at a point in the plate in the z direction; θ_x and θ_y are rotations of the normal of the plate with respect to the y- and x-axis respectively; ρ is the material density and h is the thickness of the plate; J_x and J_y are moments of inertia per unit area of the plate in the x and y directions respectively; and t denotes time. Equation (1) implies a first order shear deformation theory; the transverse shear strain is constant across the thickness of the plate.

The bending moments, twisting moment and shear forces (see Figure 3) in their respective axes and planes may be calculated from

$$M_x=-\frac{D_x}{g}\left(\frac{\partial\theta_x}{\partial x}+v_y\frac{\partial\theta_y}{\partial y}\right), \tag{2a}$$

$$M_y=-\frac{D_y}{g}\left(\frac{\partial\theta_y}{\partial y}+v_x\frac{\partial\theta_x}{\partial x}\right), \tag{2b}$$

$$M_{xy}=\frac{1}{2}D_{xy}\left(\frac{\partial\theta_y}{\partial x}+\frac{\partial\theta_x}{\partial y}\right), \tag{2c}$$

$$Q_x=D_{Qx}\left(\frac{\partial w}{\partial x}-\theta_x\right),\qquad Q_y=D_{Qy}\left(\frac{\partial w}{\partial y}-\theta_y\right). \tag{2d}$$

2.2. BOUNDARY CONDITION

The Rayleight–Ritz method dictates that only the displacement boundary conditions on the restrained edges are considered. For a fully clamped plate shown in Figure 4, the boundary conditions may be written as

$$x=0,\quad a\text{:}\qquad w=0,\qquad \theta_x=0,\qquad \theta_y=0, \tag{3a}$$

$$y=0,\quad b\text{:}\qquad w=0,\qquad \theta_x=0,\qquad \theta_y=0. \tag{3b}$$

In Figure 4, point C is the center of the plate, and points A and B are the mid-length positions of the edges at $x = 0$ and $y = 0$ respectively.

2.3. ENERGY EXPRESSIONS

The total strain energy U, the potential energy V of the external load and the kinetic energy T of the plate are respectively

$$U=\frac{1}{2}\iint_\Omega\left\{\frac{D_x}{g}\left(\frac{\partial\theta_x}{\partial x}\right)^2+\frac{D_x v_y+D_y v_x}{g}\frac{\partial\theta_x}{\partial x}\frac{\partial\theta_y}{\partial y}+\frac{D_y}{g}\left(\frac{\partial\theta_y}{\partial y}\right)^2\right.$$

$$\left.+\frac{D_{xy}}{2}\left(\frac{\partial\theta_y}{\partial x}+\frac{\partial\theta_x}{\partial y}\right)^2+D_{Qx}\left(\frac{\partial w}{\partial x}-\theta_x\right)^2+D_{Qy}\left(\frac{\partial w}{\partial y}-\theta_y\right)^2\right\}\mathrm{d}x\,\mathrm{d}y, \tag{4a}$$

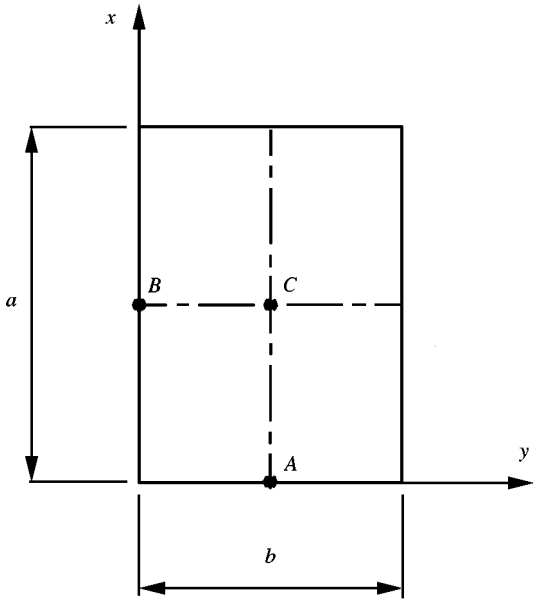

Figure 4. Rectangular orthotropic plate.

$$V = -\iint_{\Omega} pw \, dx \, dy, \tag{4b}$$

$$T = \frac{\rho h}{2} \iint_{\Omega} \left(\frac{\partial w}{\partial t}\right)^2 dx \, dy + \frac{1}{2} \iint_{\Omega} \left[J_x \left(\frac{\partial \theta_x}{\partial t}\right)^2 + J_y \left(\frac{\partial \theta_y}{\partial t}\right)^2 \right] dx \, dy, \tag{4c}$$

where the integration is over the domain Ω of the plate in the x–y plane.

2.4. ELASTIC CONSTANTS

For a conventional orthotropic plate, the elastic constants in equation (1) are

$$D_x = \frac{E_x h^3}{12}, \qquad D_y = \frac{E_y h^3}{12}, \qquad D_{xy} = \frac{G_{xy} h^3}{6}, \tag{5a}$$

$$D_{Qx} = k_s G_{xz} h, \qquad D_{Qy} = k_s G_{yz} h, \tag{5b}$$

$$v_x = v_{xy}, \qquad v_y = v_{yx} = v_{xy} \frac{E_y}{E_x}, \tag{5c}$$

where E_x and E_y are the elastic moduli, G_{xy}, G_{xz} and G_{yz} are the shear moduli, h is the thickness and v_{xy} and v_{yx} are the Poisson ratios. The parameter k_s is the transverse shear correction factor and is usually taken as $\frac{5}{6}$ or $\pi^2/12$.

If we consider an isotropic plate with bending stiffness $D = Eh^3/12(1 - v^2)$, then equations (5a) and (5b) are reduced to

$$D_x = D_y = (1 - v^2)D, \qquad D_{xy} = (1 - v)D, \qquad D_{Qx} = D_{Qy} = k_s G h. \tag{6}$$

In the analysis of symmetrical composite laminates [12], the flexural properties are usually represented by six parameters; namely, bending and twisting stiffnesses, D_{11}, D_{22}, D_{66} and D_{12}, and shear stiffnesses A_{55} and A_{44}. These parameters can be converted to the required elastic constants in Libove and Batdorf's theory by utilizing the following relationship:

$$v_x = \frac{D_{12}}{D_{22}}, \qquad v_y = \frac{D_{12}}{D_{11}}, \tag{7a}$$

$$D_x = D_{11}(1 - v_x v_y), \qquad D_y = D_{22}(1 - v_x v_y), \tag{7b}$$

$$D_{xy} = 2D_{66}, \qquad D_{Qx} = k_s A_{55}, \qquad D_{Qy} = k_s A_{44}. \tag{7c}$$

In this way, the method can be used to analyze composite laminates. Comparisons can then be made to validate the present approach.

2.5. LAGRANGIAN MULTIPLIER TECHNIQUE

Chandrashekhara *et al.* [13] adopted the Lagrangian multiplier technique for the bending analysis of cross-ply clamped laminates while Ramkumar *et al.* [9] and Chen and Ramkumar [10] used it to predict the dynamic response of clamped orthotropic plates including transverse shear. In these approaches, the displacements of the plate are assumed as

$$w = \sum_{m=1}^{M} \sum_{n=1}^{N} c_{mn} \sin\left(\frac{m\pi x}{a}\right) \sin\left(\frac{n\pi y}{b}\right), \tag{8a}$$

$$\theta_x = \sum_{m=1}^{M} \sum_{n=1}^{N} a_{mn} \cos\left(\frac{m\pi x}{a}\right) \sin\left(\frac{n\pi y}{b}\right), \tag{8b}$$

$$\theta_y = \sum_{m=1}^{M} \sum_{n=1}^{N} b_{mn} \sin\left(\frac{m\pi x}{a}\right) \cos\left(\frac{n\pi y}{b}\right), \tag{8c}$$

where the parameters c_{mn}, a_{mn} and b_{mn} are unknown coefficients and M and N are the number of series items incorporated in the analysis.

It can be seen that the trigonometric functions in equations (8b) and (8c) satisfy the boundary conditions of zero deflection and zero tangential rotations of equation (3). However, they do not satisfy the four boundary conditions of zero normal slopes at the four edges given by the second condition of equation (3a) and the third condition of equation (3b). To satisfy these boundary conditions, certain constraints related to the coefficients c_{mn}, a_{mn} and b_{mn} must be imposed. For instance, the condition $\theta_x = 0$ at $x = 0$ may be expressed, using equation (8b), as

$$\sum_{m=1}^{M} \sum_{n=1}^{N} a_{mn} \sin\left(\frac{n\pi y}{b}\right) = \sum_{n=1}^{N} \sin\left(\frac{n\pi y}{b}\right) \left[\sum_{m=1}^{M} a_{mn}\right] = 0 \tag{9}$$

Obviously, equation (9) is satisfied if the following restraint is imposed:

$$\sum_{m=1}^{M} a_{mn} = 0, \quad n = 1, 2, 3, \ldots, S. \tag{10a}$$

Similarly, restraint conditions may be derived for the other three unsatisfied boundary conditions. These may be written as

$$\sum_{m=1}^{M} a_{mn}(-1)^m = 0, \quad n = 1, 2, 3, \ldots, S, \tag{10b}$$

$$\sum_{n=1}^{N} b_{mn} = 0, \quad m = 1, 2, 3, \ldots, R, \tag{10c}$$

$$\sum_{n=1}^{N} b_{mn}(-1)^n = 0, \quad m = 1, 2, 3, \ldots, R, \tag{10d}$$

where R and S are the number of Lagrangian multipliers to be used in the solution.

Introducing the Lagrangian multipliers G_{0n} and G_{an} ($n = 1, 2, \ldots, S$) and H_{0m} and H_{bn} ($m = 1, 2, \ldots, R$), the function to be minimized for the problem is

$$\Pi = U + V - \sum_{n=1}^{S} \left(G_{0n} \sum_{m=1}^{\infty} a_{mn} \right) - \sum_{n=1}^{S} \left(G_{an} \sum_{m=1}^{\infty} a_{mn}(-1)^m \right)$$

$$- \sum_{m=1}^{R} \left(H_{0m} \sum_{n=1}^{\infty} b_{mn} \right) - \sum_{m=1}^{R} \left(H_{bm} \sum_{n=1}^{\infty} b_{mn}(-1)^n \right). \tag{11}$$

The unknown multipliers G_{0n}, G_{an}, H_{0m} and H_{bm} and the unknown coefficients c_{mn}, a_{mn} and b_{mn} are determined from a solution procedure by applying the energy method. Deflection and rotations of the plate are then computed from equation (8). Consequently, by substituting these quantities into equation (2), the bending moments, twisting moment and shearing forces are obtained. Trigonometric functions used in the method will always yield zero bending moments at the edges of the plate.

Care should be exercised to ensure that the number of Lagrangian multipliers (R and S) is equal to or smaller than M and N. Otherwise, additional constraints are implied and the accuracy of the solution is jeopardized. This may be closely examined by comparing equations (9) and (10a). These equations show that the condition of zero normal slope can be satisfied completely when R and S are equal to M and N respectively. If R and S are smaller than M and N, reasonable accuracy can be obtained because the lower-mode functions are more significant on the solution than the higher-mode functions. In the present investigation, R and S are set to M and N respectively.

3. DYNAMIC RESPONSE

3.1. NATURAL FREQUENCIES AND MODE SHAPE FUNCTIONS

A closed-form solution of natural frequencies of clamped thick plates has been presented [7]. The (m, n) order natural frequencies of the plate may be denoted as $\omega_{mn}^{(r)}$ ($r = 1$–3). The lowest frequency ($r = 1$) is the flexural mode while the two higher frequencies ($r = 2, 3$) are related to transverse shear deformations in the x and y directions respectively. Once the natural frequencies are known, the corresponding vibration modes may be readily computed. The (m, n, r) order vibration mode shape functions may be written

as

$$W_{mn}^{(r)} = W_{xm}(x)\, W_{yn}(y), \tag{12a}$$

$$\Phi_{xmn}^{(r)} = a_{mn}^{(r)}\, \Psi_{xm}(x)\, W_{yn}(y), \tag{12b}$$

$$\Phi_{ymn}^{(r)} = b_{mn}^{(r)}\, W_{xm}(x)\, \Psi_{yn}(y), \tag{12c}$$

where functions W_{xm} and ψ_{xm}, and W_{yn} and ψ_{yn} are derived from the eigenvalue problems of clamped beams in the x and y directions respectively [7]. The mode shape factors $a_{mn}^{(r)}$ and $b_{mn}^{(r)}$ are calculated by using a matrix algebraic operation of extracting the eigenvectors from the stiffness matrix.

When the plate is vibrating freely with the (m, n, r) order frequency $\omega_{mn}^{(r)}$, its motion may be described by

$$w(x, y, t) = A W_{mn}^{(r)} \cos(\omega_{mn}^{(r)} t + \varphi_0), \tag{13a}$$

$$\theta_x(x, y, t) = A \Phi_{xmn}^{(r)} \cos(\omega_{mn}^{(r)} t + \varphi_0), \tag{13b}$$

$$\theta_y(x, y, t) = A \Phi_{ymn}^{(r)} \cos(\omega_{mn}^{(r)} t + \varphi_0), \tag{13c}$$

where A denotes the vibration amplitude constant and φ_0 is the phase angle.

Substituting equation (13) into equation (1) and letting $p = 0$, the following free vibration equations are derived:

$$D_{Qx}\left(\frac{\partial^2 W_{mn}^{(r)}}{\partial x^2} - \frac{\partial \Phi_{xmn}^{(r)}}{\partial x}\right) + D_{Qy}\left(\frac{\partial^2 W_{mn}^{(r)}}{\partial y^2} - \frac{\partial \Phi_{ymn}^{(r)}}{\partial y}\right) = -\rho h (\omega_{mn}^{(r)})^2 W_{mn}^{(r)}, \tag{14a}$$

$$D_{Qx}\left(\frac{\partial W_{mn}^{(r)}}{\partial x} - \Phi_{xmn}^{(r)}\right) + \frac{D_{xy}}{2}\left(\frac{\partial^2 \Phi_{xmn}^{(r)}}{\partial y^2} + \frac{\partial^2 \Phi_{ymn}^{(r)}}{\partial x \partial y}\right) + \frac{D_x}{g}\left(\frac{\partial^2 \Phi_{xmn}^{(r)}}{\partial x^2} + \nu_y \frac{\partial^2 \Phi_{ymn}^{(r)}}{\partial x \partial y}\right) = -J_x (\omega_{mn}^{(r)})^2 \Phi_{xmn}^{(r)}, \tag{14b}$$

$$D_{Qy}\left(\frac{\partial W_{mn}^{(r)}}{\partial x} - \Phi_{ymn}^{(r)}\right) + \frac{D_{xy}}{2}\left(\frac{\partial^2 \Phi_{ymn}^{(r)}}{\partial x^2} + \frac{\partial^2 \Phi_{xmn}^{(r)}}{\partial x \partial y}\right) + \frac{D_y}{g}\left(\frac{\partial^2 \Phi_{ymn}^{(r)}}{\partial y^2} + \nu_x \frac{\partial^2 \Phi_{xmn}^{(r)}}{\partial x \partial y}\right) = -J_y (\omega_{mn}^{(r)})^2 \Phi_{ymn}^{(r)}. \tag{14c}$$

3.2. FREE VIBRATION ANALYSIS

Free vibration response of an orthotropic thick plate may be computed with initial displacement and rotations $w_0(x, y)$, $\theta_{x0}(x, y)$ and $\theta_{y0}(x, y)$, and initial velocity and angular velocities $\dot{w}_0(x, y)$, $\dot{\theta}_{x0}(x, y)$ and $\dot{\theta}_{y0}(x, y)$. By the modal superposition method, free vibration of the plate may be expressed as

$$w(x, y, t) = \sum_m \sum_n \sum_r W_{mn}^{(r)} (\xi_{mn}^{(r)} \cos(\omega_{mn}^{(r)} t) + \eta_{mn}^{(r)} \sin(\omega_{mn}^{(r)} t)), \tag{15a}$$

$$\theta_x(x, y, t) = \sum_m \sum_n \sum_r \Phi_{xmn}^{(r)} (\xi_{mn}^{(r)} \cos(\omega_{mn}^{(r)} t) + \eta_{mn}^{(r)} \sin(\omega_{mn}^{(r)} t)), \tag{15b}$$

$$\theta_y(x, y, t) = \sum_m \sum_n \sum_r \Phi_{ymn}^{(r)} (\xi_{mn}^{(r)} \cos(\omega_{mn}^{(r)} t) + \eta_{mn}^{(r)} \sin(\omega_{mn}^{(r)} t)), \tag{15c}$$

where the factors $\xi_{mn}^{(r)}$ and $\eta_{mn}^{(r)}$ determine the vibration amplitude and phase angle due to the contribution of the (m, n, r) order mode shape. These are the unknown factors of the problem. The derivation of the two factors can easily be found in textbooks on structural dynamics. The resulting expressions may be written as

$$\xi_{mn}^{(r)} = \frac{\iint_\Omega (\rho h w_0 W_{mn}^{(r)} + J_x \theta_{x0} \Phi_{xmn}^{(r)} + J_y \theta_{y0} \Phi_{ymn}^{(r)}) \, \mathrm{d}x \, \mathrm{d}y}{M_{mn}^{(r)}} \tag{16a}$$

$$\eta_{mn}^{(r)} = \frac{\iint_\Omega (\rho h \dot{w}_0 W_{mn}^{(r)} + J_x \dot{\theta}_{x0} \Phi_{xmn}^{(r)} + J_y \dot{\theta}_{y0} \Phi_{ymn}^{(r)}) \, \mathrm{d}x \, \mathrm{d}y}{\omega_{mn}^{(r)} M_{mn}^{(r)}}, \tag{16b}$$

where $M_{mn}^{(r)}$ is the (m, n, r) order mode mass of the plate and is defined as

$$M_{mn}^{(r)} = \iint_\Omega [\rho h (W_{mn}^{(r)})^2 + J_x (\Phi_{xmn}^{(r)})^2 + J_y (\Phi_{ymn}^{(r)})^2] \, \mathrm{d}x \, \mathrm{d}y.$$

3.3. FORCED VIBRATION ANALYSIS

Consider the orthotropic plate subjected to dynamic loading $p = p(x, y, t)$. By the modal superposition method, the forced vibration of the plate is expressed as

$$w(x, y, t) = \sum_m \sum_n \sum_r A_{mn}^{(r)}(t) W_{mn}^{(r)}, \tag{17a}$$

$$\theta_x(x, y, t) = \sum_m \sum_n \sum_r A_{mn}^{(r)}(t) \Phi_{xmn}^{(r)}, \tag{17b}$$

$$\theta_y(x, y, t) = \sum_m \sum_n \sum_r A_{mn}^{(r)}(t) \Phi_{ymn}^{(r)}, \tag{17c}$$

where $A_{mn}^{(r)}(t)$ is the unknown (m, n, r) order vibration function to be derived.

Substituting equation (17) into equation (1) and utilizing the relationship of equation (14), the following expressions are obtained:

$$\sum_m \sum_n \sum_r [-(\omega_{mn}^{(r)})^2 \rho h A_{mn}^{(r)}(t) - \rho h \ddot{A}_{mn}^{(r)}(t)] W_{mn}^{(r)} + p = 0, \tag{18a}$$

$$\sum_m \sum_n \sum_r [-(\omega_{mn}^{(r)})^2 J_x A_{mn}^{(r)}(t) - J_x \ddot{A}_{mn}^{(r)}(t)] \Phi_{xmn}^{(r)} = 0, \tag{18b}$$

$$\sum_m \sum_n \sum_r [-(\omega_{mn}^{(r)})^2 J_y A_{mn}^{(r)}(t) - J_y \ddot{A}_{mn}^{(r)}(t)] \Phi_{ymn}^{(r)} = 0, \tag{18c}$$

where $\ddot{A}_{mn}^{(r)}(t)$ denotes the second order derivative of the vibration function $A_{mn}^{(r)}(t)$.

In the same manner as before, multiply equation (18a) by $W_{mn}^{(s)}$, equation (18b) by $\Phi_{xmn}^{(s)}$ and equation (18c) by $\Phi_{ymn}^{(s)}$. Sum all these products and then integrate in the domain Ω. The result is a second order differential equation with respect to t of the form

$$\ddot{A}_{mn}^{(r)}(t) + (\omega_{mn}^{(r)})^2 A_{mn}^{(r)}(t) = \frac{p_{mn}^{(r)}(t)}{M_{mn}^{(r)}}, \tag{19}$$

where

$$p_{mn}^{(r)}(t) = \iint_\Omega p W_{mn}^{(r)} \, \mathrm{d}x \, \mathrm{d}y. \tag{20}$$

By using Duhamel's integral, the solution of equation (19) is

$$A_{mn}^{(r)}(t) = \frac{1}{\omega_{mn}^{(r)} M_{mn}^{(r)}} \int_0^t p_{mn}^{(r)}(\tau) \sin(\omega_{mn}^{(r)}(t - \tau))\, d\tau. \tag{21a}$$

Equation (21a) represents the response within the interval of the applied loading function. However, when the load function is zero, the response is given by

$$A_{mn}^{(r)}(t) = \xi_{mn}^{(r)} \cos(\omega_{mn}^{(r)} t) + \eta_{mn}^{(r)} \sin(\omega_{mn}^{(r)} t). \tag{21b}$$

By substituting equation (21) into (17), the forced vibration response is obtained. Dynamic bending/twisting moments and shearing forces are then calculated from equation (2).

4. FINITE ELEMENT ANALYSIS

A 3-D finite element model is essential to accurately map the response of a 3-D thin-walled sandwich panel. For this purpose, the *MARC* finite element code [14] is used in the investigation. Eight-node iso-parametric shell element with reduced integration (*element* 22 in *MARC*) is used to idealize the facing plates and core webs of the 3-D FE model. In the element formulation, the effect of transverse shear deformation is taken into account by assuming a parabolic distribution across the plate thickness.

5. NUMERICAL EXAMPLES

5.1. CONVERGENCE STUDY AND VERIFICATION

To study convergence of and to verify the proposed method, a composite laminate is examined. A four-layered cross-ply [0/90/90/0°] graphite/epoxy laminate studied by Chandrashekhara *et al.* [13] has the following material properties: $E_{11} = 21 \times 10^6$ psi, $E_{22} = 1{\cdot}4 \times 10^6$ psi, $G_{12} = G_{13} = 0{\cdot}6 \times 10^6$ psi, $G_{23} = 0{\cdot}5 \times 10^6$ psi and $v_{12} = 0{\cdot}3$. Stiffness parameters ($D_{11}, D_{22}, D_{66}, D_{12}, A_{55}$ and A_{44}) were computed from laminate theory and then converted, using equation (7), to the necessary elastic constants required for the present approach.

Two cases were investigated; one is a relatively thick laminate ($a/h = 10$) and the other is a thin laminate ($a/h = 100$). Both laminates were subjected to uniform load p. Table 1 shows the progressive convergence of the solution for central deflection and bending moment of a square ($a = b$) composite laminate with increasing values of M and N using the present approach and the Lagrangian multiplier technique (LMT). Both methods approach the final solution after a number of cycles and the final results are in good agreement. However, the proposed solution converges more rapidly using fewer items in the series function. For the beam-function series, deflection accuracy is achieved at $M = N = 9$ while the Lagrangian multiplier technique requires $M = N = 60$. In computing the bending moment at the center of the plate, the Lagrangian multiplier technique requires a much higher order of effort for the same degree of accuracy compared with the proposed approach.

It is observed that the convergence trend between the two methods is different. The present method uses a series of functions in which each function completely satisfies the boundary conditions. The functions of higher modes represent higher stiffness. Therefore,

TABLE 1

Convergence of central deflection and bending moment of a uniformly loaded laminate

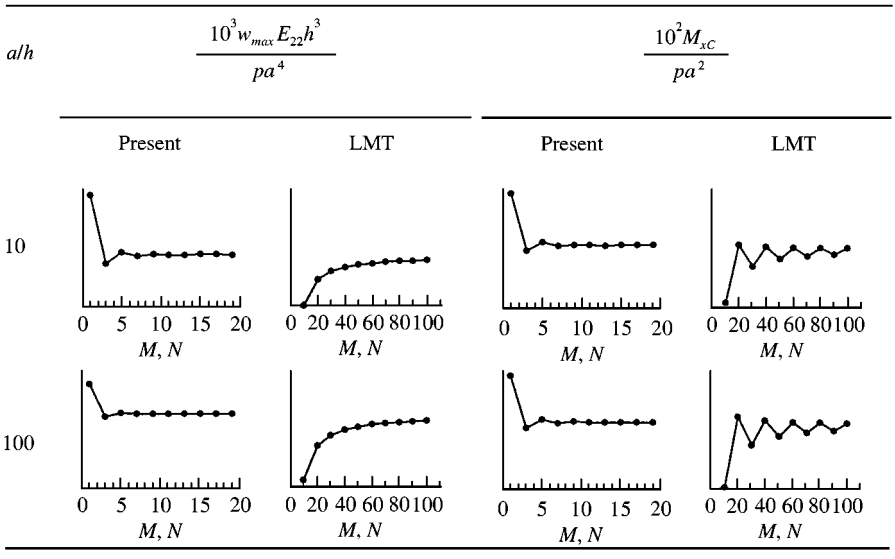

TABLE 2

Central deflection and bending moment of uniformly loaded laminates with various b/a ratios

	$\frac{10^3 w_{max} E_{22} h^3}{pa^4}$				$\frac{10^2 M_{xC}}{pa^2}$			
b/a	$a/h = 10$		$a/h = 100$		$a/h = 10$		$a/h = 100$	
	Present	LMT [13]	Present	LMT [13]	Present	LMT	Present	LMT
1·0	5·247	5·168	2·343	2·276	3·563	3·514	4·169	4·159
1·2	6·014	5·928	2·510	2·437	4·111	4·079	4·450	4·452
1·4	6·375	6·289	2·532	2·459	4·361	4·346	4·469	4·480
1·6	6·490	6·405	2·498	2·426	4·432	4·432	4·393	4·409
1·8	6·479	6·395	2·454	2·383	4·413	4·423	4·304	4·324
2·0	6·417	6·332	2·420	2·349	4·360	4·376	4·238	4·258

ignoring higher modes (small M and N values) makes the solution more flexible. The Lagrangian multiplier technique is in contrast to the above approach. The conditions imposed by the Lagrangian multiplier are excessively constrained. For instance, taking $M = N = 1$ simply gives a zero-deformation result (see equation (10)). When more modes of displacement function are included, the effect of over-constraining is relaxed and the result approaches the actual solution.

Solutions for rectangular laminates have also been obtained. Table 2 summarizes the computed central deflection and bending moment for rectangular thick and thin laminates, using the proposed approach and the Lagrangian multiplier technique. The results are in excellent agreement for all b/a ratios. Only the deflection data is available from

TABLE 3

Deflection and bending moments of square isotropic plate under uniform load

a/h	Solutions	$\frac{10^3 w_{max} D}{pa^4}$	$\frac{10^2 M_{xC}}{pa^2}$	$-\frac{10^2 M_{xA}}{pa^2}$
	Present	2·147	2·41	4·43
5	LMT	2·140	2·39	—
	FEM [15]	2·054	2·43	4·54
	Present	1·495	2·49	4·54
10	LMT	1·471	2·36	—
	FEM [15]	1·470	2·40	4·75
	Present	1·270	2·47	4·49
100	LMT	1·233	2·33	—
	FEM [15]	1·250	2·37	4·24
	Thin-plate [16]	1·260	2·31	5·13

Chandrashekhara *et al.* [13]. All the computed bending moments were derived from the proposed approach and LMT described in this paper. A program based on the LMT has been written to compute the values shown in Table 2.

In Table 2, it is observed that the difference in central deflection between the present method and LMT is always larger than the difference in bending moment. This is due to the two different convergence patterns of deflection and bending moment by LMT (see Table 1). Deflection converges smoothly while the bending moment converges erratically.

To further verify the computed central bending moment and its accuracy using the proposed method, the response of a number of square isotropic plates has been calculated. The computed maximum deflection and bending moment at the center and at mid-length of one edge (points C and A of Figure 4 respectively) are listed in Table 3. The numerical values of deflection and bending moments in Table 3, for the LMT method are computed using the program written by the authors. These results are compared with data from a triangular finite element formulation [15]. Solutions from a classical plate theory [16] are available for one case only ($a/h = 100$). It can be seen that the present method for deflection and bending moments is in excellent agreement with LMT and FEM values. As mentioned previously, the LMT yields zero bending moments at the edges of the clamped plate.

5.2. RESPONSE OF COMPOSITE LAMINATE TO IMPACT LOADING

Kant *et al.* [17] examined the dynamic response of a clamped three-layered (0/90/0°) square composite laminate of length 140 mm and thickness 4·29 mm. The material properties of the lamina are $E_{11} = 40$ GPa, $E_{22} = 8{\cdot}27$ GPa, $G_{12} = G_{23} = 4{\cdot}13$ psi, $G_{23} = 0{\cdot}03$ GPa, $v_{12} = 0{\cdot}25$ and density $\rho = 1901{\cdot}5$ kg/m^3. A load, produced by a small, cylindrical, blunt-ended projectile of diameter 9·525 mm, impinges on the center of the laminate; this load is assumed to be distributed uniformly over a circular contact area 9·525 mm in diameter. Figure 5 shows the pressure–time relationship of the loading.

The dynamic response at the center of the laminate, calculated by the proposed closed-form solution with various values of $M \times N$, is plotted in Figure 6. The proposed method agrees very well with finite element result obtained by Kant *et al.* [17]. The present

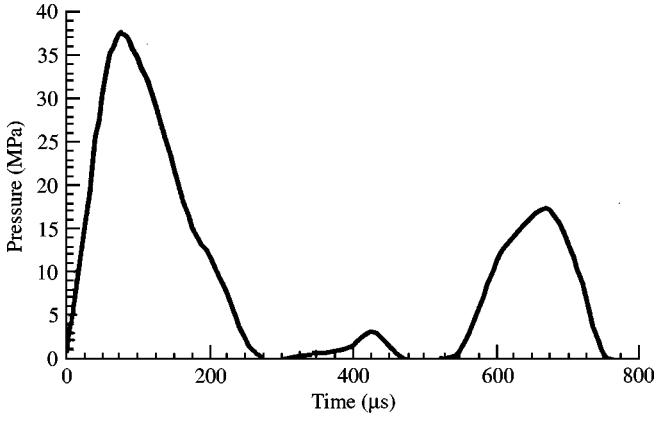

Figure 5. Applied pressure–time relationship—after Kant *et al.* [17].

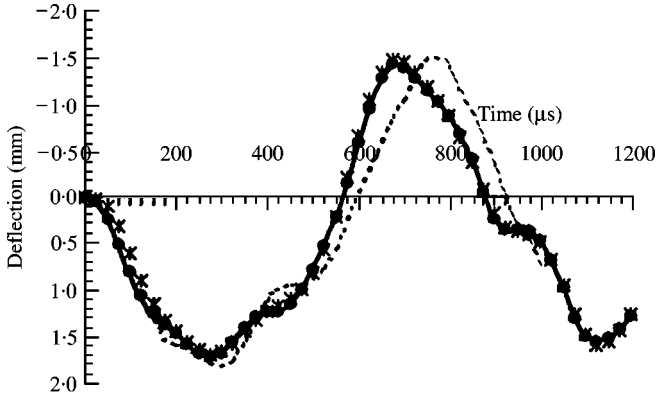

Figure 6. Central deflection response of a clamped square three-layered laminate: ——, $M = N = 15$; —●—, $M = N = 9$; —×—×—, $M = N = 3$; - - - - -, Kant *et al.* [17].

series solution gives a lower period of vibration compared with the finite element result. This is because a first order shear deformation model [11] is used in this paper whereas a higher order theory is used in the finite element formulation [17]. In the first order shear theory, a constant shear strain distribution through the thickness is assumed. This assumption makes the model stiffer than the higher order model.

5.3. DYNAMIC RESPONSE OF A TRUSS-CORE SANDWICH PANEL

The above exercises have shown conclusively that the proposed method is accurate in predicting the response of isotropic and orthotropic plates. Therefore, the dynamic response of a thin-walled truss-core sandwich panel, which is represented as an equivalent homogeneous orthotropic thick plate, can be calculated with confidence. Consider an aluminium truss-core sandwich unit with the following dimensions and properties: $p = 75$ mm, $f = 25{\cdot}91$ mm, $d = 46{\cdot}6$ mm, $t_f = 3{\cdot}4$ mm, $t_c = 2{\cdot}97$ mm, $E = 70$ GPa, $v = 0{\cdot}3$, and material density $\rho_0 = 2700$ kg/m^3.

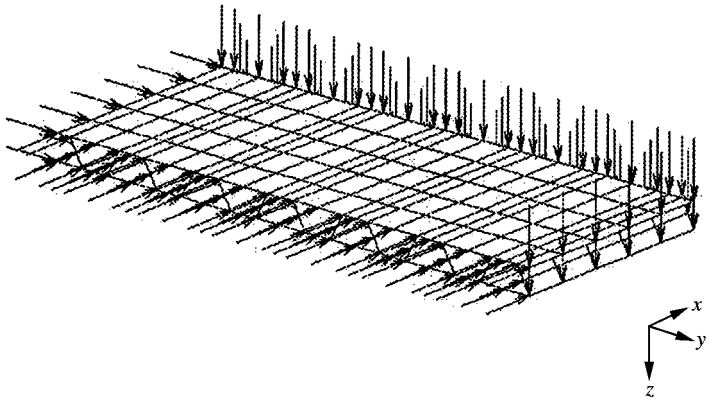

Figure 7. Three-dimensional FE model for a quarter truss-core panel.

TABLE 4

First peak central deflection of truss-core sandwich panel

Δt (ms)	Closed-form solution ($M = N = 9$)			3-D FEM analysis		
	1 mode	10 modes	20 modes	20 modes	40 modes	80 modes
0·2	1·9867	1·5793	1·5792	1·5521	1·5987	1·6036
0·02	1·9960	1·5882	1·5841	1·5639	1·6065	1·6127

Let a sandwich panel have length $a = 0{\cdot}79$ m (x direction) and width $b = 1{\cdot}9$ m (y direction). This panel size represents a household door commonly used to resist the effects of air-blast. The width implies that this panel is constructed with thirteen short truss-core sandwich units positioned side-by-side. Using the formulas in reference [5], the seven elastic constants for the truss-core panel are calculated as $D_x = 279{\cdot}55$ kN m, $D_y = 260{\cdot}19$ kN m, $D_{xy} = 198{\cdot}78$ kN m, $D_{Qx} = 43426$ kN/m, $D_{Qy} = 753{\cdot}41$ kN/m, $v_x = 0{\cdot}3$ kN m and $v_y = 0{\cdot}2792$ kN m.

Consider the panel subjected to a step-load function ($p = 150$ kPa for $t \geqslant 0$) uniformly applied on the top surface of the panel. The dynamic response may be obtained by 3-D finite element analysis using the *MARC* code [14]. Due to the symmetry of boundary condition and loading, only a quarter of the panel was modeled using 385 shell elements. Figure 7 shows the finite element mesh. The vertical arrows represent the clamped supports and the horizontal arrows denote symmetrical conditions. In the finite element computation, the mode superposition method is applied using 20, 40 and 80 modes respectively. The fundamental frequency calculated by closed-form solution is 521·67 Hz.

Forced dynamic response was determined using the present series solution taking $M = N = 9$. Three calculations were undertaken in which 1, 10, 20 modes, respectively, were involved in the mode superposition method. In both the analytical and finite element analyses, the time step was set at $\Delta t = 0{\cdot}2$ ms. This is approximately one-tenth the fundamental period. To examine the effect of the time step, refined computations were conducted by setting $\Delta t = 0{\cdot}2$ ms.

Table 4 summarizes the first peak central deflection of the panel using the two time steps. In both time-step cases, the closed-form solution converges rapidly by involving only the

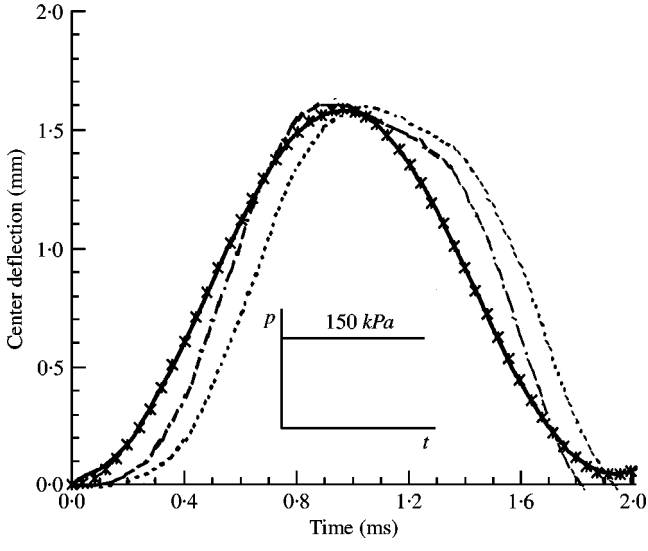

Figure 8. Dynamic response of truss-core panel subjected to step load: ——, closed-form 10 modes, $\Delta t = 0{\cdot}2$ ms; – × – × –, closed-form 10 modes, $\Delta t = 0{\cdot}02$ ms; - - - - - -, FEM 40 modes, $\Delta t = 0{\cdot}2$ ms; – · – · – · – · –, FEM 40 modes, $\Delta t = 0{\cdot}02$ ms.

first 10 modes. However, 40 modes were required in the finite element method. Figure 8 shows the computed dynamic response of the panel. Regardless of the time step used in the closed-form solution, a similar response is obtained. The finite element analysis is more sensitive to the time-step size. Although there is a slight shift in the FE response, the effect is insignificant. In both cases, the peak values are similar.

6. CONCLUSIONS

Closed-form solution for the dynamic analysis of fully clamped orthotropic thick plate and sandwich panel, including the influence of transverse shear, has been presented. Bending and forced vibration of composite laminates and isotropic plates were calculated and the results were compared with values derived from the Lagrangian multiplier technique and finite element method. The comparison validates the analytical approach and the accuracy of the closed-form solution. Consequently, the closed-form approach was used to estimate the forced response of a truss-core sandwich panel as an equivalent orthotropic thick plate continuum. The dynamic response was compared with the 3-D finite element analysis of the sandwich panel. Good agreement of the results suggests that the proposed method can be used to estimate the forced response of orthotropic plates, laminates and sandwich panels in the absence of a 3-D finite element tool.

REFERENCES

1. F. J. PLANTEMA 1966 *Sandwich Construction: The Bending and Buckling of Sandwich Beams, Plates and Shells*. New York: John Wiley & Sons.
2. C. LIBOVE and R. E. HUBKA 1951 *National Aeronautics and Space Administration* (*NASA*) *Technical Note* 2289. Elastic constants for corrugated core sandwich plates.

3. T. C. FUNG, K. H. TAN and T. S. LOK 1993 *Proceedings of the Third International Offshore & Polar Engineering Conference* (CO, USA), Vol. 4, 244–249. Analysis of C-core sandwich plate decking.
4. T. C. FUNG, K. H. TAN and T. S. LOK 1994 *American Society of Civil Engineers Journal of Structural Engineering* **120**, 3046–3065. Elastic constants for Z-core sandwich panels.
5. T. S. LOK, Q. H. CHENG and L. HENG 1999 *Proceedings of the ninth International Offshore & Polar Engineering Conference* (Brest, France), Vol. 4, 292–298. Equivalent stiffness parameters of truss-core sandwich panel.
6. T. S. LOK and Q. H. CHENG 2000 *American Society of Civil Engineers Journal of Structural Engineering* **126**, 552–559. Elastic stiffness properties and behavior of truss-core sandwich panel.
7. T. S. LOK and Q. H. CHENG 2000 *Journal of Sound and Vibration* **229**, 311–327. Free vibration of clamped orthotropic sandwich panel.
8. P. A. A. LAURA and R. DURAN 1975 *Journal of Sound and Vibration* **42**, 129–135. A note on forced vibrations of a clamped rectangular plate.
9. R. L. RAMKUMAR, P. C. CHEN and W. J. SANDERS 1987 *American Institute of Aeronautics and Astronautics Journal* **25**, 146–151. Free vibration solution for clamped orthotropic plates using Lagrangian multiplier technique.
10. P. C. CHEN and R. L. RAMKUMAR 1987 *American Institute of Aeronautics and Astronautics Journal* **25**, 316–323. Static and dynamic analysis of clamped orthotropic plates using Lagrangian multiplier technique.
11. C. LIBOVE and S. B. BATDORF 1948 *National Advisory Committee for Aeronautics* (*NACA*) *Technical Note* 1526. A general small-deflection theory for flat sandwich plates.
12. J. E. ASHTON and J. M. WHITNEY 1970 *Theory of Laminated Plates*. Stamford, CT: Technomic.
13. K. CHANDRASHEKHARA, A. H. YAHYAVI and P. R. RAO 1990 *Composite Structures* **2**, 169–179. Bending of cross-ply laminated clamped plates using Lagrange multipliers.
14. MARC ANALYSIS RESEARCH CORPORATION 1997 *MARC K*7.1 *documents Vol. B. Element Library*.
15. G. R. BHASHYAM and R. H. GALLAGHER 1983 *Computer Methods in Applied Mechanics and Engineering*, Netherlands **40**, 309–326. A triangular shear-flexible finite element for moderately thick laminated composite plates.
16. S. TIMOSHENKO and S. WOINOWSKY-KRIEGER 1959 *Theory of Plates and Shell*. New York: McGraw-Hill.
17. T. KANT, J. H. VARAIYA and C. P. ARORA 1990 *Computers and Structures* **36**, 401–420. Finite element transient analysis of composite and sandwich plates based on a refined theory and implicit time integration schemes.